Dynamics of a Flexible Passive Space Array

John V. Breakwell*
Stanford University, Stanford, Calif.
and
Gerry. B. Andeen†
Stanford Research Institute, Menlo Park, Calif.

A passive space communicator in synchronous orbit will consist of small aluminum beads chained together and aligned vertically by the Earth's gravity gradient. The analysis for small deviations from vertical uses a continuous-chain model, and pitch and roll frequencies and mode shapes are described with and without the attachment of substantial end masses. An end mass with appreciable moment of inertia can provide effective damping of the lowest-order, otherwise rigid and undamped, modes. The distortion of the chain by solar radiation pressure is estimated, assuming undesirable variations in the mass-to-area ratio of beads and end masses.

I. Introduction

THIS paper describes a new type of passive communication satellite under development. The satellite consists of an in-line array of scattering elements whose electrical principle is described by Yater[1] and illustrated in Figs. 1 and 2. Response to an electromagnetic signal at the design frequency is a scattering diffraction lobe in the form of a thin-walled cone returned to Earth. There are multiple user and antijam features, in addition to the passive nature, which make the satellite an attractive communications link or navigational aid.

We shall be discussing a test satellite whose scattering elements are 10^4 1-cm-diam aluminum spheres with an 0.5-cm separation. The test satellite is designed for near 10-GHz operation and will be in synchronous orbit. Good reception requires that the 150-m length of the array remain straight to within a few centimeters. Orbital drift, as well as several degrees of slow libration about the local vertical, can be accommodated by adjusting the transmission frequency.

For launch, the array is coiled in a container. Deployment consists in driving the array out of the container, one end first. If the scattering elements were supported by a wire, the array would retain an unacceptable residual curvature. A freely jointed, bead-chain construction, on the other hand, would rely on the rather weak gravity gradient at synchronous altitude for straightening. Some inaccuracy, however, in deployment could result in an initially tumbling motion, and, as this tumbling motion is slowed by damping (see later), there will be periods of compression rather than tension in the chain (see Fig. 3), which could result in the chain tying itself into knots. A happy compromise consists in a support structure of about 100 sections of relatively stiff wire connected by joints that are free up to about 3° of motion (see Fig. 4). Residual curvature of the sections is now tolerable, and knotting is impossible. Gravity gradient and damping can be relied upon to align and straighten the array.

An important feature of the gravity-gradient environment is that a chain can undergo even large motions without departing from straightness. This is quite unlike the behavior of a hanging chain in a constant gravity field, where damping in the joints can be relied on to damp the attitude motion. Attitude or libration damping in a gravity gradient thus requires special treatment.

In this paper, we deal with: 1) the motion of a chain in the gravity-gradient environment, including tip arrangements designed to damp the attitude motion; and 2) the effect of solar radiation pressure on array straightness when the solar force on the scattering elements varies because of size or surface differences. The design shown in Fig. 4 meets two additional criteria not discussed: 1) that mutual gravitation effects be small compared with the gravity gradient; and 2) that the gravity-gradient effect be greater than any solar pressure forces so that the Earth-pointing, stable equilibrium position is guaranteed even in the case of sun directly overhead.

The work reported here models the array as a cable with continuous flexibility and is limited to a small-motion, linearized analysis. In a parallel program, a computer simulation has been developed using a finite-element model that includes the nonlinearities. Simulated behavior is as predicted for small motions.

II. Analytical Formulations

Coordinates and the Equation of Motion

We use a reference frame attached to the center of mass of the cable. This reference frame moves in a circular orbit of

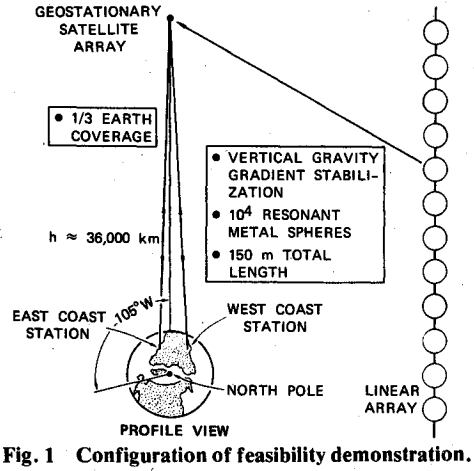

Fig. 1 Configuration of feasibility demonstration.

Presented at the AIAA/ASME/SAE 17th Structures, Structural Dynamics, and Materials Conference, King of Prussia, Pa., May 5-7, 1976 (in bound volume of Conference papers, no paper number); submitted Oct. 28, 1976; revision received March 18, 1977.

Index categories: Satellite Communication Systems (including Terrestrial Stations); Spacecraft Configuration and Structural Design (including Loads); Spacecraft Dynamics and Control.

*Professor of Astronautics. Fellow AIAA.

†Senior Research Engineer.

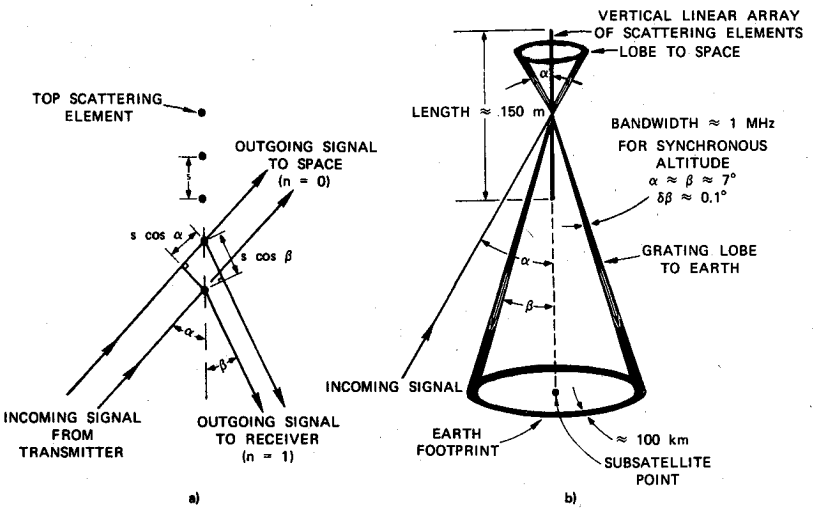

Fig. 2 Response of a linear array of isotropic scatters.

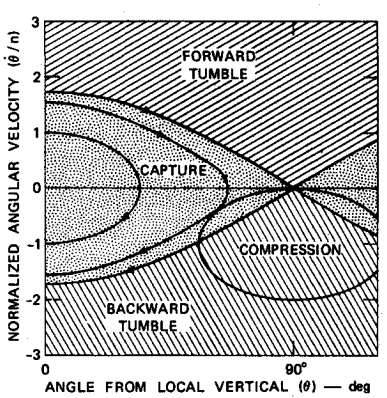

Fig. 3 Phase-plane plot for the in-plane motion of a rigid rod.

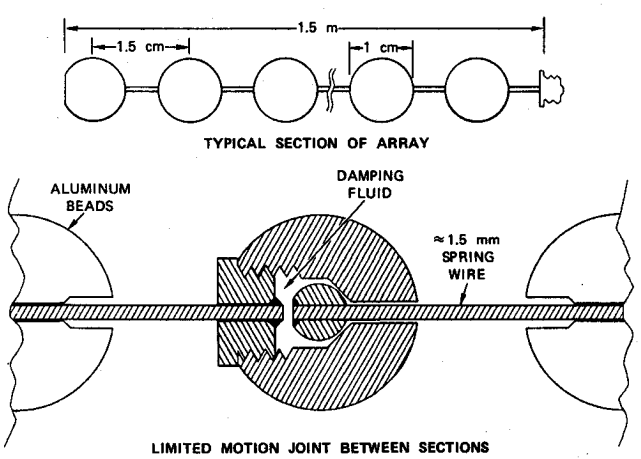

Fig. 4 Array construction.

radius r, as shown in Fig. 5. The x axis (with unit vector $\boldsymbol{i}$) is defined by the direction of the radius vector from the center of the Earth, the y axis (with unit vector $\boldsymbol{j}$) lies in the orbital plane, and the z axis (with unit vector $\boldsymbol{k}$) is perpendicular to the orbit plane.

We consider the motion of a uniform, perfectly flexible cable or chain. The equation of motion for an array element, ds, located at position $\boldsymbol{\rho}$ with respect to the origin of the chosen reference system, can be written as

$$\sigma ds[\ddot{\boldsymbol{\rho}}+2(\boldsymbol{nk}\times\dot{\boldsymbol{\rho}})+\boldsymbol{nk}\times(\boldsymbol{nk}\times\boldsymbol{\rho})] = n^2\sigma ds[3(\boldsymbol{i}\cdot\boldsymbol{\rho})\boldsymbol{i}-\boldsymbol{\rho}] + [\text{string-tension terms}] + [\text{radiation-pressure terms}] \quad (1)$$

where

s = length along the array
σ = linear density
n = orbital rate
$\boldsymbol{\rho}$ = position vector

Small-Amplitude Approximations

If the cable is nearly straight and in a nearly vertical position $dx \cong ds$, and the position vector can be approximated by

$$\boldsymbol{\rho} \cong x\boldsymbol{i}+y(x,t)\boldsymbol{j}+z(x,t)\boldsymbol{k} \quad (2)$$

then the bracket, noted previously as string-tension terms, can be written as

$$\left[\frac{dT}{dx}\boldsymbol{i}+\frac{d}{dx}\left(T\frac{dy}{dx}\right)\boldsymbol{j}+\frac{d}{dx}\left(T\frac{dz}{dx}\right)\boldsymbol{k}\right]dx \quad (3)$$

where T is the cable tension. Furthermore, we can assume that the cable tension is near its equilibrium value and that this tension is nearly independent of the cable displacement. Thus, a linearized differential equation for the equilibrium tension T_e can be written as

$$\frac{dT_e}{dx} = -3n^2x\sigma \quad (4)$$

The solution of this equation depends on boundary conditions, which for the free cable are zero tension at its ends. Hence, we obtain

$$T_e = 3/2\sigma n^2[(L/2)^2 - x^2] \quad (5)$$

where L is the total length of the array.

The components of the vector equation (1) now can be written explicitly to give the desired equations for the natural motion for the cable in the absence of radiation pressure. The equation for the component in the $\boldsymbol{i}$ direction shows that the tension depends on $\dot{y}$; however, for small deflections this term is small, and the tension may be replaced by its equilibrium value in the $\boldsymbol{j}$ and $\boldsymbol{k}$ components to yield

$$\ddot{y} = \frac{3}{2}n^2\left[\left(\frac{L}{2}\right)^2 - x^2\right]\frac{d^2y}{dx^2} - 3n^2x\frac{dy}{dx} \quad (6)$$

$$\ddot{z} = \frac{3}{2}n^2\left[\left(\frac{L}{2}\right)^2 - x^2\right]\frac{d^2z}{dx^2} - 3n^2x\frac{dz}{dx} - n^2z \quad (7)$$

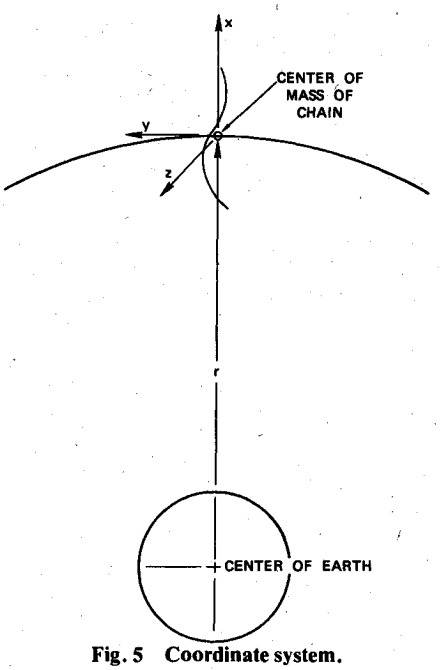

Fig. 5 Coordinate system.

Equations (6) and (7) are separable in the independent variables x and t. The following harmonic forms are obtained:

$$y(x,t)=e^{j\omega t}y(x) \tag{8}$$

$$z(x,t)=e^{j\omega t}z(x) \tag{9}$$

Normalization of the Equations of Motion

The equations of motion of the cable depend on its tension, which is a function of the tip arrangement. Therefore, it would be advantageous to normalize these equations in such a way that the tip arrangement affects only the boundary conditions. This approach suggests a normalization based on the variable ξ, given by

$$\xi=x/a \tag{10}$$

where a is the distance to a zero tension point, which may be outside the array. Using this variable, the differential equations for the shape functions of the harmonic solution can be written as

$$(1-\xi^2)\frac{d^2y}{d\xi^2}-2\xi\frac{dy}{d\xi}+\frac{2\omega^2}{3n^2}y=0 \tag{11}$$

$$(1-\xi^2)\frac{d^2z}{d\xi^2}-2\xi\frac{dz}{d\xi}+\frac{2}{3}\left(\frac{\omega^2}{n^2}-1\right)z=0 \tag{12}$$

The cable tension and normalization variable for three cases (no tip masses, a single tip mass, and two equal tip masses) are shown in Fig. 6. In the case of the free cable,

$$a=L/2 \tag{13}$$

and the boundary conditions are y, z finite at $\xi=\pm 1$.

The mode shapes are Legendre polynomials, $y_l(\xi)=z_l(\xi)=P_l(\xi)$, and the corresponding natural frequencies ω are given by

$$(\omega_y/n)^2=(\omega_z/n)^2-1=3/2l(l+1) \tag{14}$$

The lowest mode shapes, corresponding to $l=1$, are straight, and the various modes are shown in Fig. 7.

Viscous Damping of the Higher Modes

Viscous damping in the loose joints between the wire sections may be treated approximately in our continuous

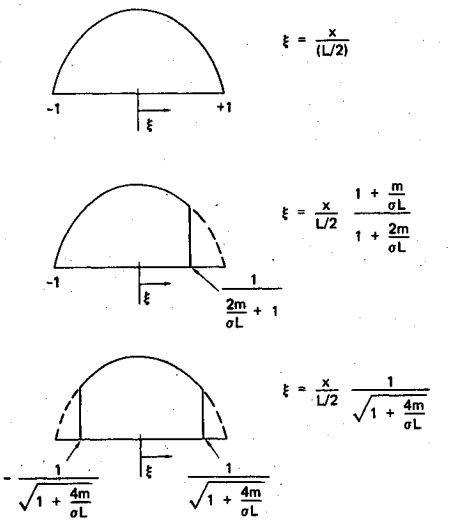

Fig. 6 Array tension for various configurations.

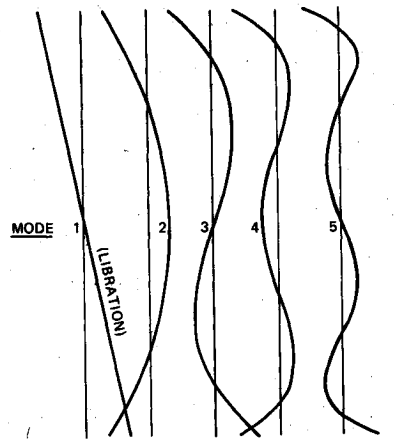

MODE	FREQUENCY	
	in plane	out of plane
1	1.73 n	2.0 n
2	3.00 n	3.16 n
3	4.24 n	4.36 n
4	5.48 n	5.57 n
5	6.71 n	6.78 n
	$n\sqrt{\frac{3}{2}\,i(i+1)}$	$n\sqrt{1+\frac{3}{2}\,i(i+1)}$

n – ORBITAL RATE
i – MODE NUMBER

Fig. 7 Gravity-gradient normal modes for free cable.

model by a bending moment proportional to the rate of change of curvature. For in-plane motion, for example,

$$M=k\dot{y}_{xx}\cong k\dot{\theta}/l \tag{15}$$

where l is 1.5 m, and θ is the bend in the joint. The partial differential equation for the chain now becomes

$$(1-\xi^2)y_{\xi\xi}-2\xi y_\xi+2/3(\omega/n)^2y=j\eta y_{\xi\xi\xi\xi}$$

where

$$\eta=\frac{2}{3}\,\frac{k\omega}{\sigma n^2(L/2)^4}$$

The boundary conditions are $y_{\xi\xi}=y_{\xi\xi\xi}=0$ at $\xi=\pm 1$, and the appropriate mode shapes and damped frequencies can be found numerically. For small η, the rate of loss of energy in the higher modes ($l>1$) can be calculated from the mode shapes for the undamped case $\eta=0$:

$$\text{rate of loss of energy} = 3/8\eta\omega\sigma L n^2 A^2 \int_{-1}^{1} P_l'^2(\xi)\,d\xi \qquad (16)$$

where A is the amplitude of the lth mode, $y_l(\xi)=AP_l(\xi)$. This is equivalent to a complex change in the natural frequency:

$$\frac{2}{3}\left(\frac{\omega_y}{n}\right)^2 = l(l+1)+j\eta\left(\tfrac{l+2}{4}\right)(2l+1)(l^2+l+3) \qquad (17)$$

The slight change in mode shapes, predominantly near the free ends, is given by following the composite expansion, in which w denotes $(1-\xi)/(j\eta)^{1/3}$:

$$\frac{y}{A} = P_l(\xi) - (j\eta)^{2/3}K_2\int_w^\infty A(w')\,dw'$$
$$+j\eta\left\{\frac{K_l}{2}P_l(\xi)\ell n(1-\xi^2)+Q_{l-2}(\xi)-\frac{K_l}{2}\ell n w\right.$$
$$+K_l\left[\int_0^w B(w')\,dw'-0.7933\right]+K_3\int_w^\infty A(w')\,dw'$$
$$+K_2\left[\frac{3}{20}A'(w)-\frac{1}{10}w^2A(w)-\frac{l(l+1)}{2}\right.$$
$$\left.\left.\times\left(w\int_w^\infty A(w')\,dw'+\frac{1}{2}A'(w)\right)\right]\right\}+O(\eta^{4/3}) \qquad (18)$$

where Q_{l-2} is an easily found polynomial, and where

$$K_l=\binom{l+2}{4}(l^2+l+3) \qquad K_2=\frac{P_l''(1)\Gamma(1/3)}{6^{1/3}\Gamma(2/3)}$$
$$K_3=l(l+1)-\frac{1}{5}\frac{P_l''(1)\Gamma^2(1/3)}{6^{2/3}\Gamma^2(2/3)}$$

and the functions $A(w)$, $B(w)$ are defined by

$$A''(w)=2wA(w) \qquad B''(w)=2wB(w)-1$$
$$A(0)=1 \qquad B'(0)=0$$
$$A(+\infty)=0 \qquad B(+\infty)=0$$

Effect of Tip Masses

For one tip mass at the upper end of the array, the distance to the zero tension point is

$$a=\frac{L}{2}\left[\frac{1+(2m/\sigma L)}{1+(m/\sigma L)}\right] \qquad (19)$$

and the upper boundary condition is $y_{\xi\xi}=z_{\xi\xi}=0$ at $\xi=1/[1+(2m/\sigma L)]$. For two equal tip masses,

$$a=(L/2)\sqrt{1+(4m/\sigma L)} \qquad (20)$$

and the boundary conditions are $y_{\xi\xi}=z_{\xi\xi}=0$ at $\xi=\pm 1/\sqrt{1+(4m/\sigma L)}$. The effect of one or two tip masses is to raise the frequencies of all except the lowest-mode $l=1$, and the modified mode shapes and frequencies can be obtained numerically. Generally, for small tip masses m^+, $m^- \ll \sigma L$, $\xi_{\max}\cong 1-(2m^+/\sigma L)$, $\xi_{\min}\cong -1+(2m/\sigma L)$, and the approximate mode shapes are obtainable analytically:

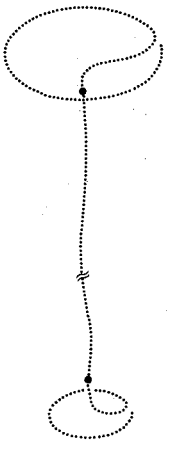

Fig. 8 Array of inertial tips.

$$\left.\begin{matrix} y \\ \text{or} \\ z \end{matrix}\right\} = A\left\{P_l(\xi)+\epsilon\left[Q_{l-2}^*(\xi)+\frac{1}{4l+2}P_l(\xi)\ell n(1-\xi^2)\right]\right.$$
$$\left.-\epsilon'\frac{P_l(\xi)}{2l+1}\int_0^\xi\frac{d\xi'}{(1-\xi'^2)[P_l(\xi')]^2}+O(\epsilon^2)\right\} \qquad (21)$$

where Q_{l-2}^* is another polynomial, and

$$\frac{2}{3}\left(\frac{\omega_y}{n}\right)^2-l(l+1)=\frac{2}{3}\left[\left(\frac{\omega_z}{n}\right)^2-1\right]-l(l+1)$$
$$=\epsilon=4(2l+1)P_l'(1)\frac{(m^+)^2+(m^-)^2}{(\sigma L)^2} \qquad (22)$$

and

$$\epsilon'=4(2l+1)P_l'(1)\frac{(m^+)^2-(m^-)^2}{(\sigma L)^2} \qquad (23)$$

the parameter ϵ gives the increase in frequencies for $l>1$.

Libration Damping with Tip Inertias

To obtain damping of the lowest (straight) modes, "inertial tips" are included whose natural libration frequencies differ from that of a long, thin, rigid body. These tips may be obtained by circular wire formations, as in Fig. 8. For the purposes of analysis, each tip is idealized as an axisymmetric rigid body. It is joined to the chain, as in Fig. 9, by a viscous damper, a straight wire of length L_l and density σ_l per unit length, and a loose joint, which, like the damper, is assumed to permit large deflections, e.g., up to 60°. The dynamic equations for the tip are

$$I_z\ddot{\theta}=-3n^2(I_z-I_x)\theta-bT\theta+bY-K(\dot{\theta}-\dot{\theta}_l) \qquad (24a)$$

$$m(\ddot{y}+L_l\ddot{\theta}_l+b\ddot{\theta})=-Y \qquad (24b)$$

$$(\sigma_l L_l^3/12)(\ddot{\theta}_l+3n^2\theta_l)=-(L_l/2)(T+T_l)\theta_l$$
$$+(L_l/2)(Y+Y_l)+k(\dot{\theta}-\dot{\theta}_l) \qquad (24c)$$

$$\sigma_l L_l[\ddot{y}+(L_l/2)\ddot{\theta}_l]=Y-Y_l \qquad (24d)$$

$$Y_l=T_l y' \qquad (24e)$$

where k is a measure of the viscous damping.

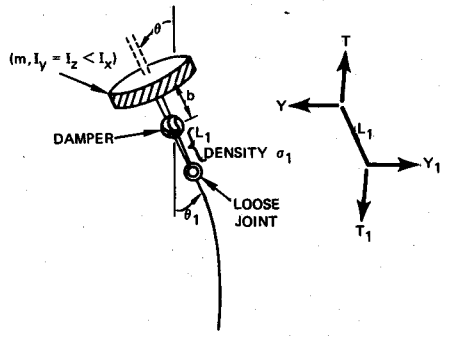

Fig. 9 Dynamic model of tip inertia.

Assuming that the lengths b, L_1 are much smaller than the chain length L, the dynamic equations in the neighborhood of the rigid frequency $n\sqrt{3}$ may be approximated by

$$\begin{bmatrix} mb\frac{L}{2} - I_x + jk'\sqrt{3} & mb\frac{L}{2} - I_x \\ -2jk'\sqrt{3} & \left(m + \frac{\sigma_1 L_1}{2}\right) L_1 L \end{bmatrix} \begin{bmatrix} \theta - \theta_1 \\ \theta_1 - y' \end{bmatrix} = \begin{bmatrix} I_x y' \\ 0 \end{bmatrix} \tag{25}$$

where $k' = k/3n$, and

$$(m+\sigma_1 L_1)\left[\frac{L}{2}y' - \left(1+\frac{\epsilon}{2}\right)y\right]$$

$$= mb(\theta-\theta_1) + \left[m(L_1+b) + \frac{\sigma_1 L_1^2}{2}\right](\theta_1 - y') \tag{26}$$

where $\epsilon = \frac{2}{3}[(\omega_y/n)^2 - 3]$.

Equation (25) describes the motion of the tip forced by a straight libration of the chain, and Eq. (26) then provides a boundary condition for the chain which will provide a slight deviation from straightness, as well as some damping of the libration. Hence,

$$y = A[\xi + (\epsilon/6)\xi \ln(1-\xi^2)] \tag{27}$$

where the imaginary part of ϵ, which provides the damping, is given approximately by

$$\frac{\vartheta m \epsilon}{6\xi_M(1-\xi_M)} = \frac{4jI_x^2 k'\sqrt{3}}{L^2(m+\sigma_1 L_1)Q} \tag{28}$$

and

$$Q = \left(mb\frac{L}{2} - I_x\right)^2 + 3k'^2\left[1 - \frac{I_x - mb(L/2)}{[m+(\sigma_1 L_1/2)](L_1 L/2)}\right]^2$$

where ξ_M denotes $\xi_{\max}$. Efficient damping is obtained if the lengths b and L_1 are chosen so that $mb(L/2) - I_x$ is positive and not large, whereas

$$1 - \frac{I_x - (mbL/2)}{[m+(\sigma_1 L_1/2)](L_1 L/2)} = 0$$

Suppose, then, that

$$I_z \cong \tfrac{1}{2} I_x \tag{29}$$

Choose

$$mb(L/2) = \tfrac{3}{4} I_x \tag{30a}$$

$$[m + (\sigma_1 L_1/2)] L_1 L = \tfrac{1}{2} I_x \tag{30b}$$

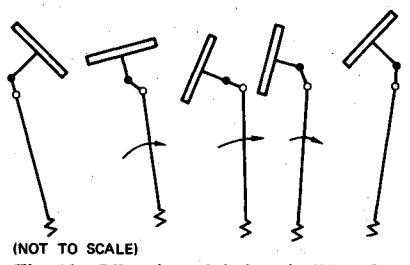

Fig. 10 Libration of tip inertia (½ cycle).

and suppose that

$$k' = I_x/(4\sqrt{3}) \tag{31}$$

Then

$$\theta - \theta_1 \cong -4y' \tag{32a}$$

$$\theta_1 - y' \cong -4jy' \tag{32b}$$

so that the tip libration is substantially greater than that of the chain, thereby exercising the damping (see Fig. 10). Theoretically it would be possible to obtain much larger amplification, but the tip motion soon would grow beyond the range where the linear approximation is meaningful! A similar analysis applies to the out-of-plane motion. For a pair of tip inertias in the form of rings, radius $5m$, in-plane libration decreases by a factor of 2 in 5½ days and out-of-plane libration in slightly less time (having the same damping ratio).

Distortion by Radiation Pressure

We turn now to the effect of variations in the radiation pressure acceleration from sphere to sphere. The partial differential equations for the distortions are

$$(1-\xi^2)y_{\xi\xi} - 2\xi y_\xi + \tfrac{2}{3}(\omega/n)^2 y = -\tfrac{2}{3}(F_y/n^2) \triangleq f_y(\xi) \tag{33}$$

$$(1-\xi^2)z_{\xi\xi} - 2\xi z_\xi = \tfrac{2}{3}[(\omega/n)^2 - 1]z = -\tfrac{2}{3}(F_z/n^2) \triangleq f_z(\xi) \tag{34}$$

where $\omega/n = 1$ for the in-plane distortion, and $\omega/n = 0$ for the out-of-plane distortion, ignoring small higher harmonic components due to shadowing for certain seasons of the year. Here F_y, F_z denote the radiation pressure forces per unit mass.

The in-plane forced solution is expressible as

$$y(\xi) = y_1(\xi)y(0) + y_2(\xi)y_\xi(0) + \int_0^\xi [y_2(\xi)y_1(\zeta) - y_1(\xi)y_2(\zeta)] f_y(\zeta)\,d\zeta \tag{35}$$

where $y_1(\xi)$ and $y_2(\xi)$ are solutions of the homogeneous equations corresponding to

$$y_1(0) = 1 \quad y_2(0) = 0$$

$$y_{1\xi}(0) = 0 \quad y_{2\xi}(0) = 1$$

The appropriate displacement $y(0)$ and slope $y_\xi(0)$ at the c.m. are determined by the tip boundary conditions:

$$[\tfrac{2}{3}y - 2\xi y_\xi]_{\pm\xi_M} = f_y(\pm\xi_M) \tag{36}$$

in which the small effect (ϵ) due to tip inertia has been neglected. The deviation from straightness is given by

$$\eta(\xi) = y(\xi) - \frac{1}{2\xi_M}\int_{-\xi_M}^{\xi_M} y(\xi)\,d\xi - \frac{3\xi}{4\xi_M^3}\int_{-\xi_M}^{\xi_M} \xi y(\xi)\,d\xi \tag{37}$$

which can be expressed in the form

$$\eta(\xi) = A(\xi)s(\xi_M) + B(\xi)D(\xi_m) + \int_0^{\xi_M} [K_1(\xi,\zeta)s(\zeta) + K_2(\xi,\zeta)D(\zeta)]\,d\zeta \tag{38}$$

where $s(\xi)$ and $D(\xi)$ denote the sum and difference:

$$s(\xi) = f_y(\xi) + f_y(-\xi) \tag{39a}$$

$$D(\xi) = f_y(\xi) - f_y(-\xi) \tag{39b}$$

In particular, if the radiation pressure acceleration were 5% higher than nominal on all of the spheres in the central portion of the chain, but 5% lower on all of the spheres near the ends, the deviaiton from straightness would be approximately 1 m, which is excessive. However, this is a very pessimistic hypothesis, and statistical reasoning leads to a much lower estimate of this deviation. Thus, the mean-square deviation at position ξ is

$$E\{\eta^2(\xi)\} = 2\sigma_{f_y}^2 \left\{ A^2(\xi) + B^2(\xi) + \xi_c \int_0^{\xi_M} [K_1^2(\xi,\zeta) + K_2^2(\xi,\zeta)]\,d\zeta \right\} \tag{40}$$

where ξ_c is a (small) nondimensional correlation length, equal in our case to l/a (where l is 1.5 m), and $\sigma_{f_y}^2$ is the mean-square deviation in f_y for the 1.5-m section, 0.01 of that for a single sphere.

The rms deviation is

$$\sigma_\eta = \left\{ \frac{1}{\xi_M} \int_0^{\xi_M} E\{\eta^2(\xi)\}\,d\xi \right\}^{1/2} \tag{41}$$

Computation reveals that a 5% rms fluctuation in the radiation pressure acceleration of these spheres yields an rms deviation σ_η of less than 2 mm. The out-of-plane distortion can be analyzed similarly and will be even smaller.

III. Conclusions

A passive communication satellite consisting of jointed sections of wire with suitable scattering elements appears to be feasible. Capture from tumbling and ultimate damping to a sufficiently straight, Earth-pointing configuration appear to be possible with the aid of tip inertias. The distortion of the chain by solar radiation pressure, because of undesirable variations in the mass-to-area ratios of beads and end masses, is quite small. A more serious consequence of the radiation pressure, as pointed out by Batdorf,[2] is the partial shadowing of spheres in the main chain but not in the tip inertias when the sun is almost overhead, and the reverse effect when the local time is approximately 6 a.m. or 6 p.m. It has been estimated that, if the damping in the viscous joints of the chain is sufficiently small, the forced response due to shadowing includes a once-daily deviation with amplitude 40 cm, the higher components being unimportant. If damping in the viscous joints does not reduce the three-times-daily deviation appreciably, it may be necessary to increase the spacing between the spheres.

Acknowledgment

Support for this work has been provided by the Defense Advanced Research Projects Agency through the Defense Communications Agency, Contract DCA 100-74-C-0035.

References

[1] Yater, J. C., "Signal Relay Systems Using Large Space Arrays," *IEEE Transactions on Communications*, Vol. COM-20, Dec. 1972, pp. 1108-1121.

[2] Batdorf, S. B., private communication.